iScience, Volume *24*

Supplemental information

YAP regulates alveolar epithelial cell differentiation and *AGER* via NFIB/KLF5/NKX2-1

Jason J. Gokey, John Snowball, Anusha Sridharan, Parvathi Sudha, Joseph A. Kitzmiller, Yan Xu, and Jeffrey A. Whitsett

Figure S1

Gate Strategy

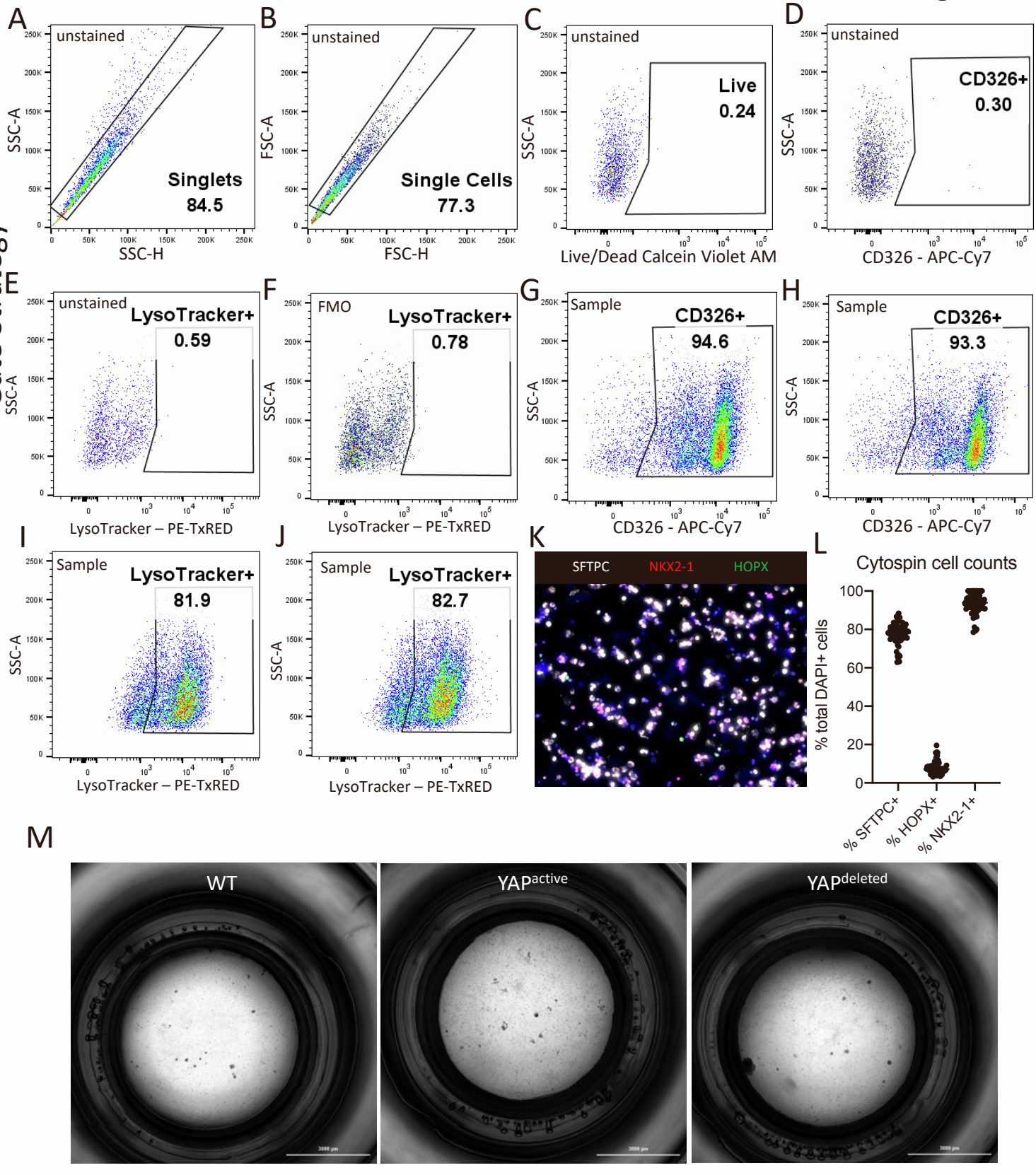

Figure S1: Gating strategy to test the purity of alveolar epithelial cell enrichment, related to Figure 3. Alveolar epithelial cells were isolated from wild-type (*Stk3*$^{flox/flox}$*Stk4*$^{flox/flox}$) (N=2) and subjected to FACS analysis utilizing Calcein Violet AM to detect live cells (cells had greater than 95% viability), CD326+ to identify epithelial cells and CD326+/LysoTracker+ cells to quantify AT2 cells. A-F.) Representative examples of side scatter, forward scatter, unstained samples, and LysoTracker FMO to establish gating strategy. G,H) Analysis of CD326+ cells demonstrating greater than 93% epithelial cells from the isolated cells. I,J) Analysis of CD326+/LysoTracker+ cells demonstrating greater than 80% AT2 cell population in isolated cells. K) Representative 20X image of immunofluorescence analysis of SFTPC, HOPX, and NKX2-1 on cytospins of isolated cells. L) Quantification of SFTPC+, HOPX+, and NKX2-1+ cells, each point of the graph represents analysis of a 20X image of cells isolated from N=2 mice, 36 images from each cytospin. M) Brightfield microscope images showing whole wells of organoid cultures generated with PND14 WT, YAP^{active}, and YAP^{deleted} AT2 cells co-cultured with PND14 WT fibroblasts after 21 days of culture.

AT1 Transcriptional Network

Figure S2

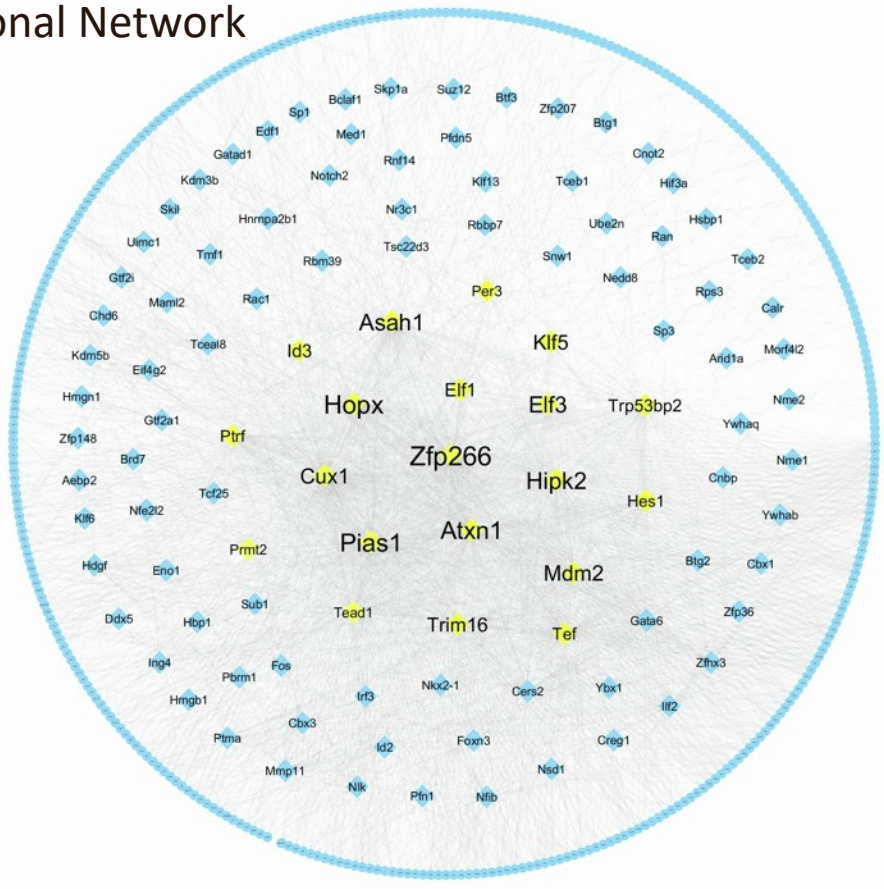

AT2 Transcriptional Network

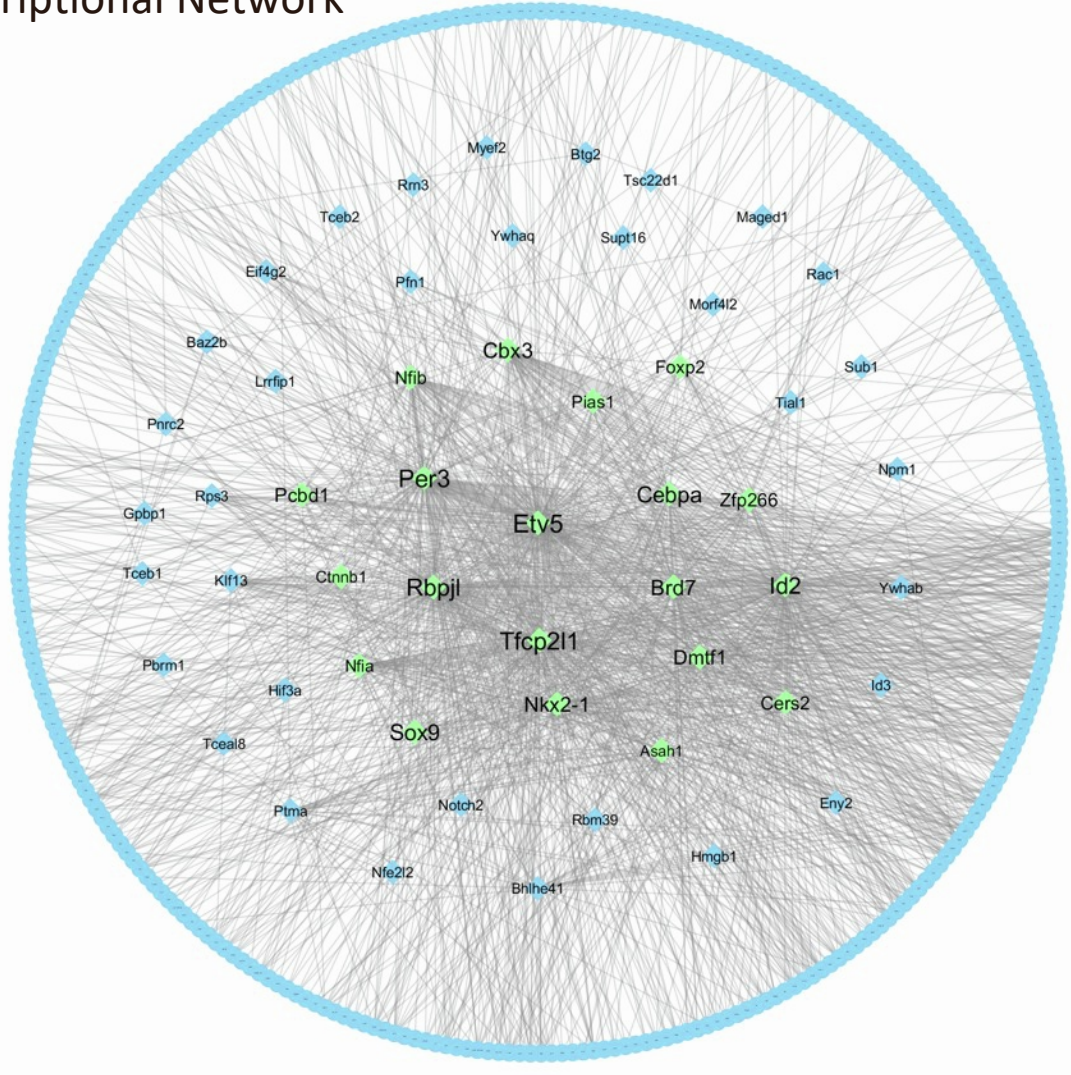

Figure S2: Transcriptional Regulatory Networks of predicted upstream drivers of gene changes associated with AT1 and AT2 cell differentiation, related to Figure 4.

Figure S3

A)

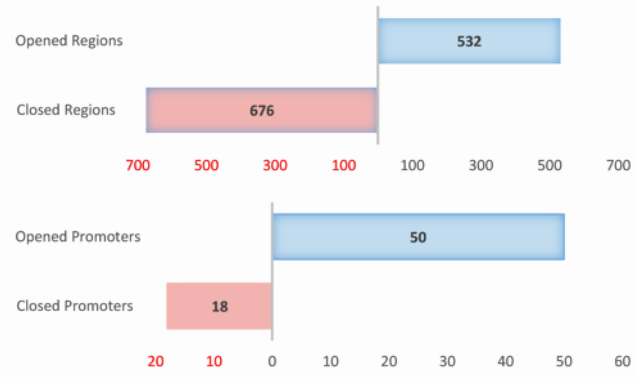

B)

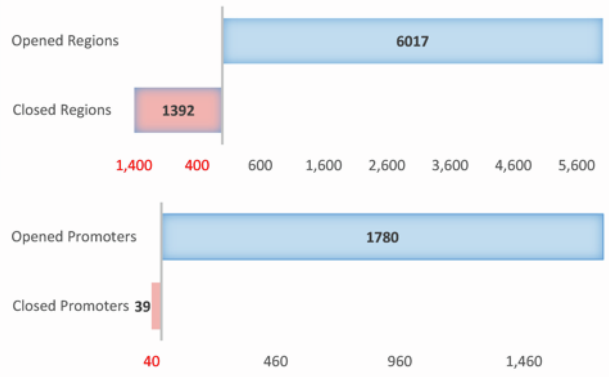

C)

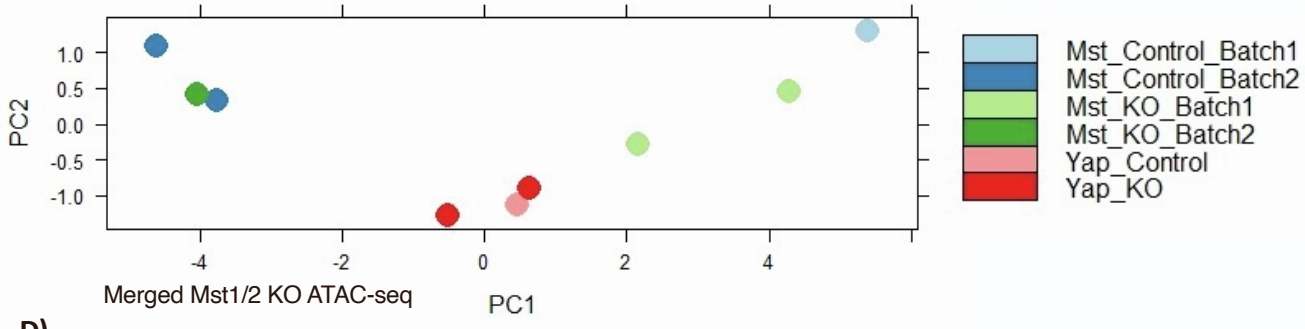

D)

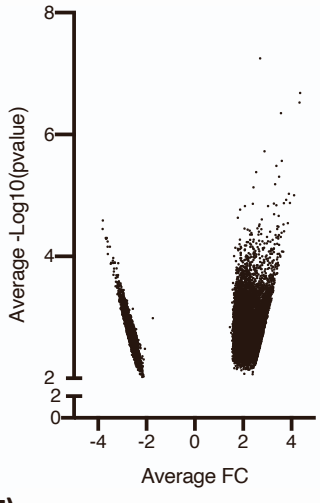

E)

Genotype	TSS Enrichment Score	Total Peaks	Reads in Peaks	Reads	FRiP Score
Yap_KO	35.6	325729	10503165	24556540	0.427714
Yap_KO	30.6	154323	10476400	34762346	0.301372
WT_Mst	12.1	144939	4466472	28657540	0.155857
WT_Yap	29.4	410930	10952407	27221458	0.402345
Mst_KO	16.3	513385	8320863	24228006	0.34344
Mst_KO	18.4	135778	3271935	10906510	0.299998
MSt_KO_Batch2	49	178122	10216412	19381712	0.527116
Wt_Mst_Batch2	52.5	195591	12501421	20793019	0.601232
Wt_Mst_Batch2	48.7	196644	11585819	21038466	0.550697

F)

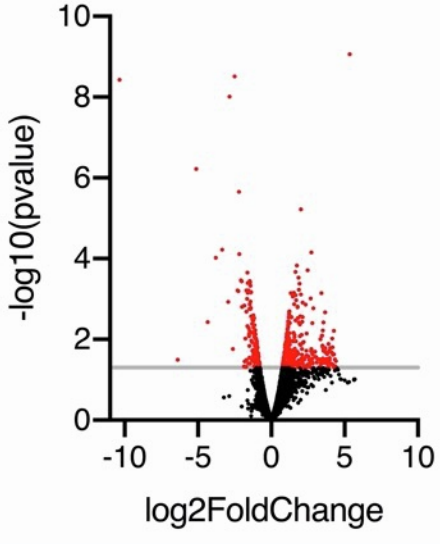

G)

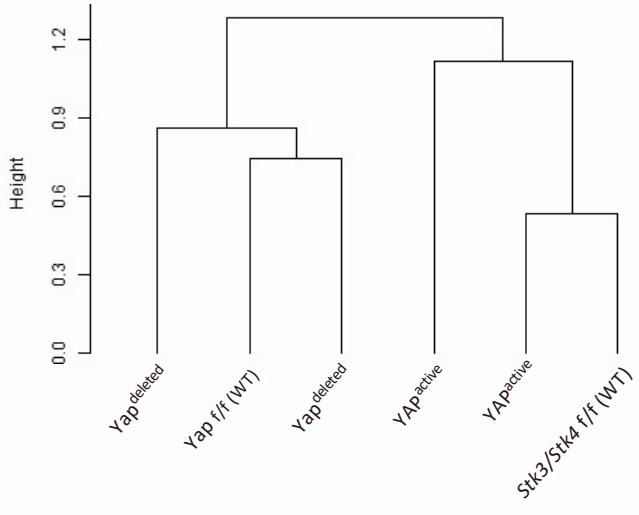

Figure S3: Chromatin accessibility in epithelial cells isolated from $YAP^{deleted}$ mice related to Figure 5 and Figure 7. A) ATAC-seq analyses of $YAP^{deleted}$ lung epithelium, by Homer, showed few changes in DNA accessibility after YAP deletion. B) An identical Homer analysis of YAP activated lung epithelial cells shows increased DNA accessibility. ATAC-seq analyses were performed on EPCAM+ cells comparing $YAP^{deleted}$ mice (N=2) to a littermate control. Only regions opened in both mutant replicates were considered significant. Analysis of WT littermates shows background differences in *Yap*$^{flox/flox}$ and *Stk3*$^{flox/flox}$*Stk4*$^{flox/flox}$ control mice. ATAC-seq and RNA-seq was performed on EPCAM+ lung cells isolated from controls mice of both $YAP^{deleted}$ and YAP^{active} backgrounds. YAP activation opened the chromatin accessibility of 1780 promoters in initial 1 vs 1 comparison. Further samples were assessed for Figure 7A. C.) PCA plot of ATAC-seq from individual samples shows the different clustering between batches of samples, therefore requiring individual analysis of each batch of samples. D.) Volcano plot of opened and closed promoters in YAP active mice. E.) Quality control assessment of TSS enrichment score, total peaks, reads, and FRIP score for each ATAC-seq sample. F.) A volcano plot of the 467 differentially expressed genes ($p<.05$, $FC>1.5$) show baseline differences between the two backgrounds. G.) Hierarchal clustering of open DNA coding regions showed control mice cluster better with their mutant littermates.

Analysis of genes downregulated in YAP^{active} mice

Category	Name	p-value	Hit Count in Query List	Hit Count in Genome
GO: Biological Process	Mesenchyme development	7.4E-06	13	312
GO: Cellular Component	Extracellular matrix	3.92E-05	17	598
ToppCell Atlas	Lungmap Lungmap - Mouse FluidigmC1 Fibroblast	6.21E-11	55	1840
ToppCell Atlas	Lungmap Mouse Lung PND1 MyoFB Subtype MyoFB-A	1.15E-10	19	243

Table S1: Biological processes associated with genes downregulated in YAP^{active} AT2 cells, related to Figure 6.

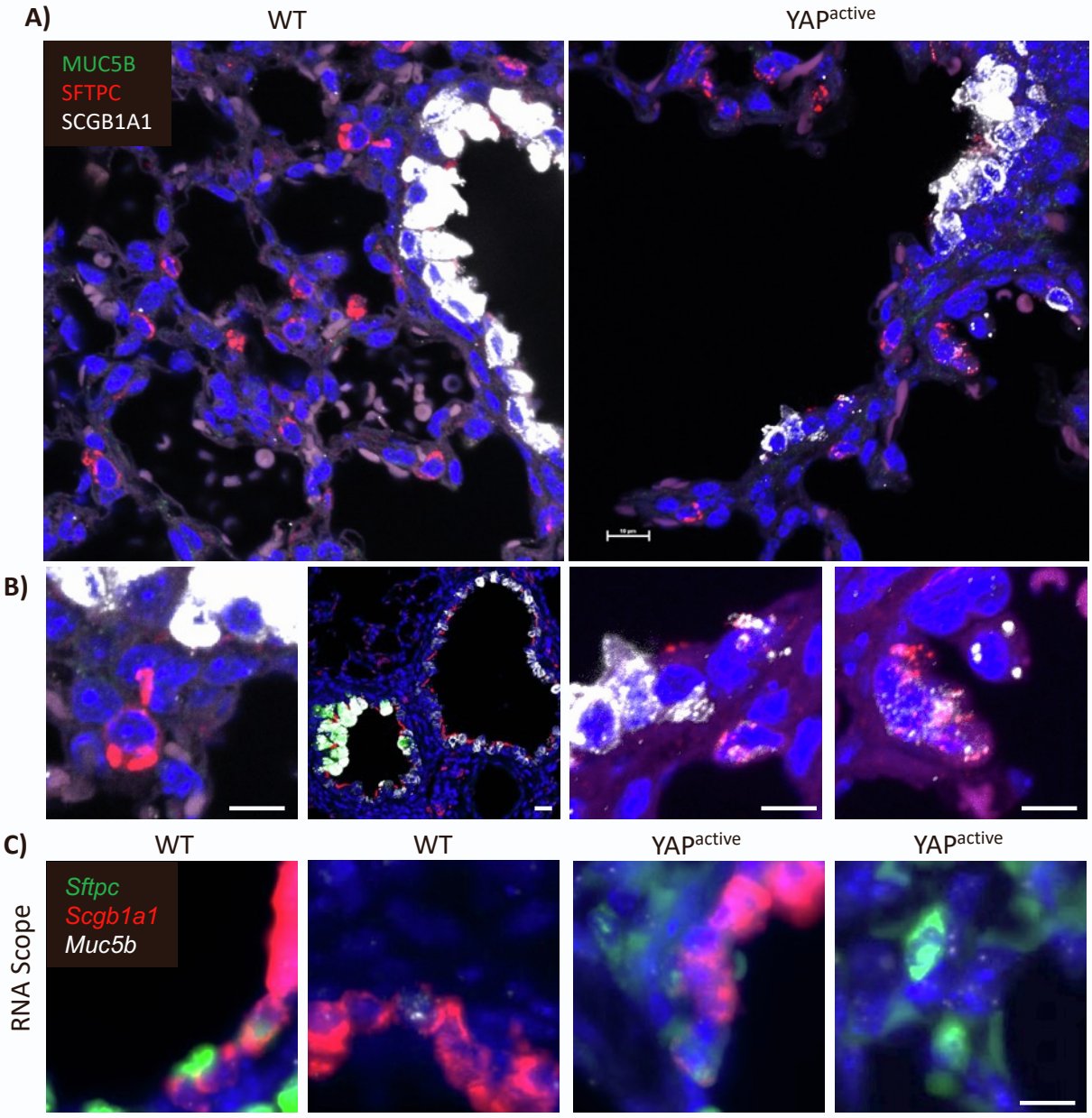
A)
WT
YAPactive
MUC5B
SFTPC
SCGB1A1
B)
C)
WT
WT
YAPactive
YAPactive
RNA Scope
Sftpc
Scgb1a1
Muc5b

Figure S4: Immunofluorescence images of proximal markers in AT2 cells, related to Figures 6. A,B.) Immunofluorescence staining of MUC5B (green), SFTPC (red), and SCGB1A1 (white) demonstrates co-localization of SFTPC and SCGB1A1 but not MUC5B in epithelial cells in YAP^{active} mice. C.) RNAscope fluorescent in-situ hybridization of *Muc5b, Scgb1a1,* and *Sftpc* demonstrating the presence of potential BASC cells and the localization of *Muc5b* in WT and YAP^{active} mice.

Figure S5

A)

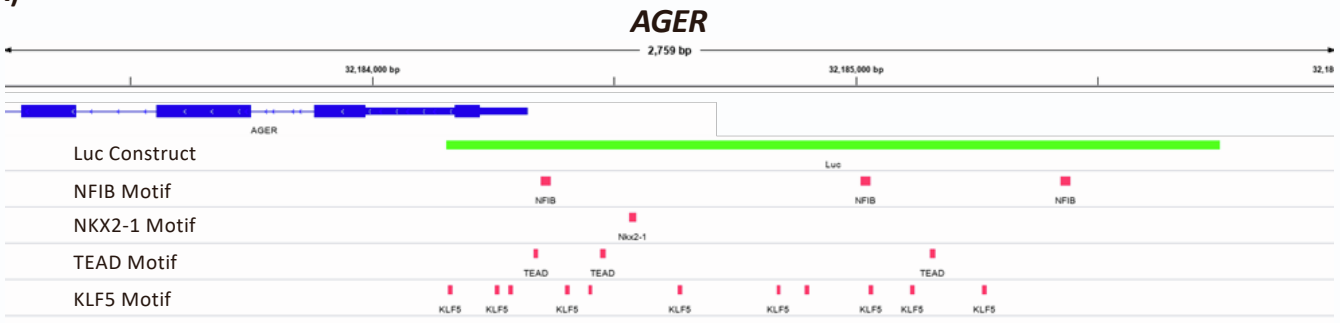

B)

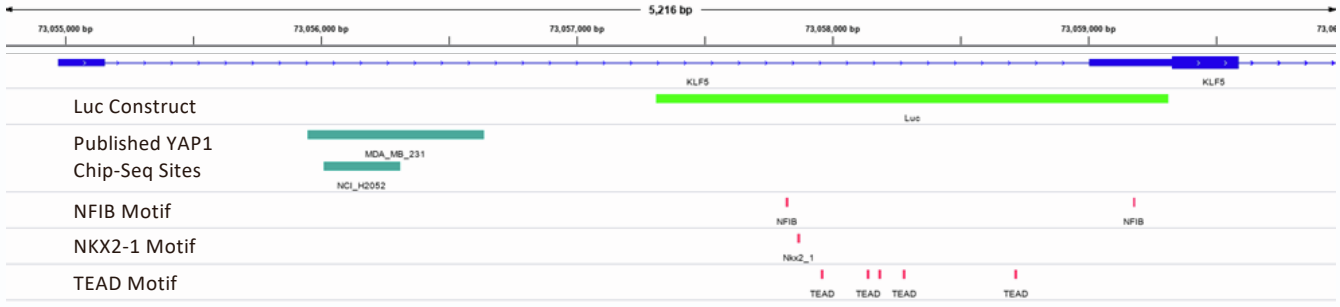

C)

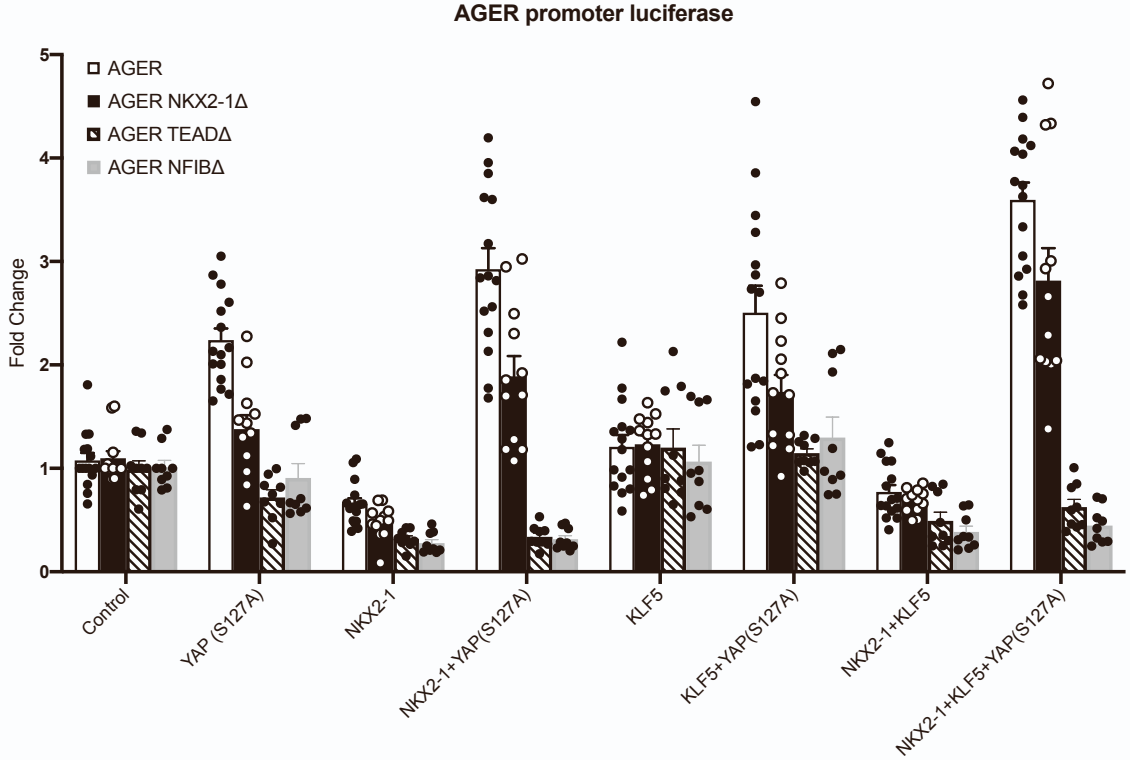

Figure S5: *KLF5* and *AGER* promoter regions have consensus KLF5, TEAD, NKX2-1, and NFIB binding sites, related to Figure 7. Luciferase promoter analyses of *KLF5* and *AGER*, genes induced in YAP^{active} mice, identify motifs for transcription factors predicted to regulate AT1 and AT2 differentiation. A) The genomic location of the *Ager* promoter used for the luciferase construct is shown (green) with the location of consensus NFIB, NKX2-1, TEAD and KLF5 DNA binding sites located in close proximity. B) The location of the *KLF5* promoter used for the luciferase construct is shown (green) with previously reported YAP1 ChIP-seq binding sites (turquoise). Locations of NKX2-1, TEAD and NFIB potential binding sites are shown (red). Consensus DNA binding sites were identified using Meme suite's Fimo package, $p < .0005$. C.) Full analysis of increased luciferase promoter activity in *AGER* luciferase assay with site mutagenesis in NFIB, NKX2-1, and TEAD predicted binding sites in the presence of YAP, NKX2-1, and KLF5 expression.

Figure S6

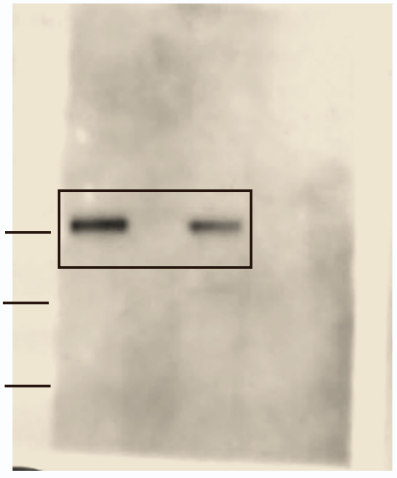

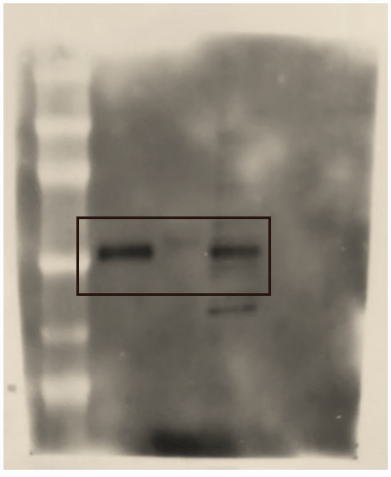

NFIB

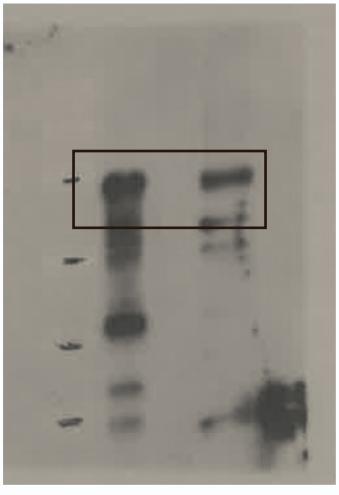

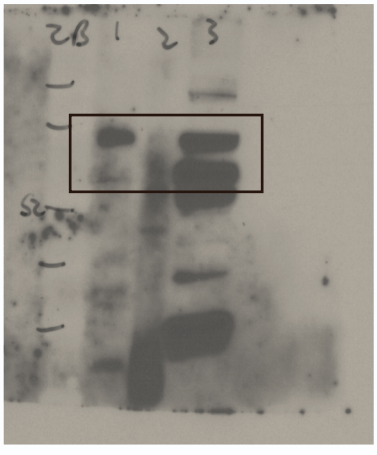

YAP (S127A)

Figure S6: Full blots of the gels for the immunoprecipitation assays from Figure 8 are shown. Regarding the ladder locations, images are scans of blots imaged on film, with the film subsequently overlayed on the blot and marker lines were drawn in to mark ladder locations.